Oxidation resistance mechanism of Si-Cr press hardening steel with Si and Cr alloy elements

Xia Pu[1,a], Cong Long[2,b], Xiangxing Deng[2], Jian Wang[2], Lintao Gui[2], Jinsheng Zhang[1], Zhibai Wang[1], Xiaomin Xu[1], Yan Zhao[2,c,†], Hongzhou Lu[3,d] and Yangwei Wang[4]

[1]*Chongqing Changan Automobile Co., Ltd, Chongqing, 401120, China*
[2]*Chongqing Innovation Center, Beijing Institute of Technology, Chongqing, 401120, China*
[3]*CITIC Metal Co., Ltd., Beijing, 100004, China*
[4]*Beijing Institute of Technology, Beijing, 100081, China*
Email: [a]puxia@changan.com.cn, [b]lc3220221331@163.com,
[c,†]yan.zhao11@icloud.com, [d]luhz@citic.com

Press hardening steel (PHS) is widely used in the production of automotive components. However, the traditional 22MnB5 steel, during the heating and hot stamping process, tends to develop a substantial amount of loose and easily detachable oxide scale on the surface, negatively impacting the lifespan of molds and the quality of forming. To address this issue, this work designed PHS with different component ratios (Si, Cr, Ni, Cu, and Mo) based on the composition of 22MnB5. High-temperature oxidation tests were conducted on the designed steels under conditions of 930°C withholding times ranging from 5 to 30 minutes. The results highlight that the Si-Cr composite PHS exhibits the most remarkable resistance to oxidation. Microscopic characterization and phase analysis of the oxide layer structure reveal the formation of a Si-Cr enrichment layer between the matrix and the oxide layer, consisting of Fe_2SiO_4 and $FeCr_2O_4$. This dense enrichment layer, tightly binds to the matrix, hindering the outward diffusion of Fe from the matrix. The Si-Cr steel demonstrates an 88% reduction in oxide weight gain compared to 22MnB5 steel. This research would provide insights for the future development of PHS in the automotive industry, particularly in addressing challenges associated with oxide scale formation during the heating and hot stamping processes.

Keywords: PHS; Si-Cr addition; Oxidation resistance mechanism; Fe_2SiO_4; $FeCr_2O_4$.

1. Introduction

Hot pressing forming technology is widely used in the production of automotive parts, with 22MnB5 being the currently prevalently hot-pressing-forming-steel (PHS)[1-3]. While the forming process of parts using 22MnB5 is relatively mature, the uncoated 22MnB5 exhibits poor oxidation resistance leading to the formation of a significant oxide layer during the hot-pressing process. The oxide layer tends to detach during production, necessitating frequent mold cleaning, which not only reduces production efficiency, but also shortens

† This work was supported by the Development of Composite Micro-alloying Press Hardening Steel and Application in the Lightweight Dump Truck Project of CITIC Group (Grant Number 2022FWNB-30137), Major Scientific and Technological Innovation Project of CITIC Group (Grant Number 2022zxkya06100) and Development of Coating-free and Shot Blasting-free Press Harding Steel Project from Changan Automobile (Grant Number Q10 230575).

Y. Zhang and M. Ma (eds.), *Proceedings of the 7th International Conference on Advanced High Strength Steel and Press Hardening (ICHSU 2024)*, Atlantis Highlights in Materials Science and Technology 3,
https://doi.org/10.2991/978-94-6463-581-2_40

the mold's service life. Additionally, industrial production requires an extra shot blasting process to remove the oxide scale from the surface of uncoated 22MnB5 plates, contributing environmental pollution. To address these challenges, the conventional approach involves depositing an Al-Si coating on the surface of 22MnB5 to enhance oxidation resistance[4-7]. However, Al-Si coated plates incur high costs and are prone to sticking to rollers, thus prolonging the production cycle and increasing costs. Therefore, researchers have explored antioxidant composition design and process parameter control to reduce oxide layer thickness, improve oxide layer density and adhesion to matrix, and ultimately enhance material oxidation resistance, thereby reducing surface treatment costs. Zhao et al. reported that it's the oxidation resistance of 22MnB5 was effectively improved by adding Cr and Si alloy elements[8]; Zhang et al. also proved that Cr and Si can improve the oxidation resistance of 22MnB5[9]; Zhang et al[10] and Deng et al[11] explored the effect of Mo element on the oxidation resistance of steel. However, these studies primarily focused on the effect of alloying elements on the oxidation resistance without considering their cost implications in practical industrial application. This study aims to design a new composition based on 22MnB5, conduct oxidation weight gain experiments, characterize the microstructure of the oxide layer, determine the optimal composition ratio, and further explore the oxidation resistance mechanism of the new type of PHS.

2. Experimental Materials and Methods

In this study, we optimize the composition of components based on 22MnB5. The design principles were as follows: 1. Explore the optimal composition design for reducing oxidation weight gain and improving adhesion of oxide layer, while considering the existing hot stamping process of PHS; 2. Minimize the use of alloying elements to reduce costs while ensuring antioxidant effectiveness. According to the national standard GB/T 13303, high-temperature oxidation weight gain experiments were conducted on the designed steel grade. Materials were prepared by vacuum melting furnace (SRL-2000) and processed into cuboid samples (30*10*3mm^3), and the scale and impurities on the surface were polished with sandpaper (1500CW). After cleaning with ultrasonic cleaning instrument (040SD), the samples were heated at 930 ℃ for 5min and 10min in a heating furnace (SX-ES12123) and cooled to room temperature in the air. The mass before oxidation experiment (m_1) and the mass after oxidation experiment (m_2) of each sample were measured using an electronic balance with an accuracy of 0.001g. The size of the sample before the oxidation experiment was measured using vernier caliper with accuracy of 0.01mm, and the area (S) was calculated. Three parallel samples were used in each experiment, and the oxidation weight gain ratio and weight gain per unit area were calculated accordingly.

Composition optimization was conducted into two stages: The first stage involved exploring the influence of adding single elements on the oxidation resistance of 22MnB5. According to the existing research, three typical elements (Si, Cr, Ni), known to improve the oxidation resistance of steel were selected, and different contents of three elements were added to the composition design. In the second stage, the comprehensive influence of

the mold's service life. Additionally, industrial production requires an extra shot blasting process to remove the oxide scale from the surface of uncoated 22MnB5 plates, contributing environmental pollution. To address these challenges, the conventional approach involves depositing an Al-Si coating on the surface of 22MnB5 to enhance oxidation resistance[4-7]. However, Al-Si coated plates incur high costs and are prone to sticking to rollers, thus prolonging the production cycle and increasing costs. Therefore, researchers have explored antioxidant composition design and process parameter control to reduce oxide layer thickness, improve oxide layer density and adhesion to matrix, and ultimately enhance material oxidation resistance, thereby reducing surface treatment costs. Zhao et al. reported that it's the oxidation resistance of 22MnB5 was effectively improved by adding Cr and Si alloy elements[8]; Zhang et al. also proved that Cr and Si can improve the oxidation resistance of 22MnB5[9]; Zhang et al[10] and Deng et al[11] explored the effect of Mo element on the oxidation resistance of steel. However, these studies primarily focused on the effect of alloying elements on the oxidation resistance without considering their cost implications in practical industrial application. This study aims to design a new composition based on 22MnB5, conduct oxidation weight gain experiments, characterize the microstructure of the oxide layer, determine the optimal composition ratio, and further explore the oxidation resistance mechanism of the new type of PHS.

2. Experimental Materials and Methods

In this study, we optimize the composition of components based on 22MnB5. The design principles were as follows: 1. Explore the optimal composition design for reducing oxidation weight gain and improving adhesion of oxide layer, while considering the existing hot stamping process of PHS; 2. Minimize the use of alloying elements to reduce costs while ensuring antioxidant effectiveness. According to the national standard GB/T 13303, high-temperature oxidation weight gain experiments were conducted on the designed steel grade. Materials were prepared by vacuum melting furnace (SRL-2000) and processed into cuboid samples (30*10*3mm^3), and the scale and impurities on the surface were polished with sandpaper (1500CW). After cleaning with ultrasonic cleaning instrument (040SD), the samples were heated at 930 ℃ for 5min and 10min in a heating furnace (SX-ES12123) and cooled to room temperature in the air. The mass before oxidation experiment (m_1) and the mass after oxidation experiment (m_2) of each sample were measured using an electronic balance with an accuracy of 0.001g. The size of the sample before the oxidation experiment was measured using vernier caliper with accuracy of 0.01mm, and the area (S) was calculated. Three parallel samples were used in each experiment, and the oxidation weight gain ratio and weight gain per unit area were calculated accordingly.

Composition optimization was conducted into two stages: The first stage involved exploring the influence of adding single elements on the oxidation resistance of 22MnB5. According to the existing research, three typical elements (Si, Cr, Ni), known to improve the oxidation resistance of steel were selected, and different contents of three elements were added to the composition design. In the second stage, the comprehensive influence of

weight loss still exceeds50% when the content reaches2.0%; Conversely, increasing Ni content has the least obvious effect on enhancing oxidation resistance. Furthermore, samples P1-3, P1-4 and P1-8 suggest that, based on the similar element content increases, the weight loss effect follows the order of Si > Cr > Ni. Surface quality observations after oxidation experiment are shown in Fig 2. Samples P1-4 (1.0Cr) and P1-8 (1.0Ni) show obvious scale peeling, blistering and discoloration.

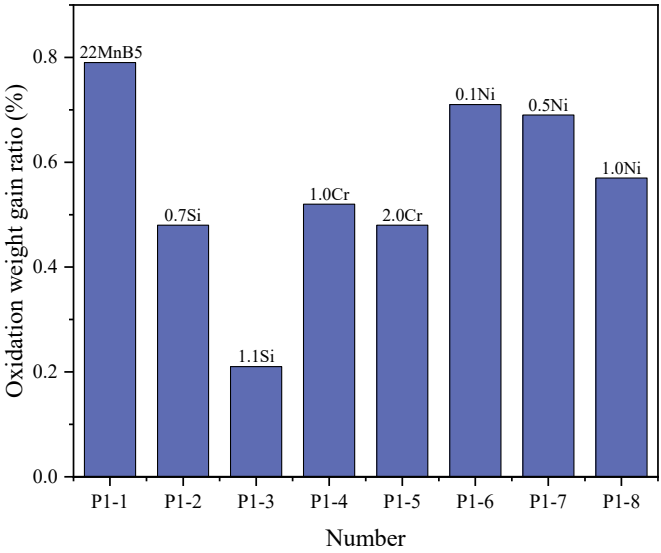

Fig. 1 Oxidation weight gain ratio of single alloy elements (Holding temperature: 930 ℃; Heat preservation time: 10 min; Atmosphere: air)

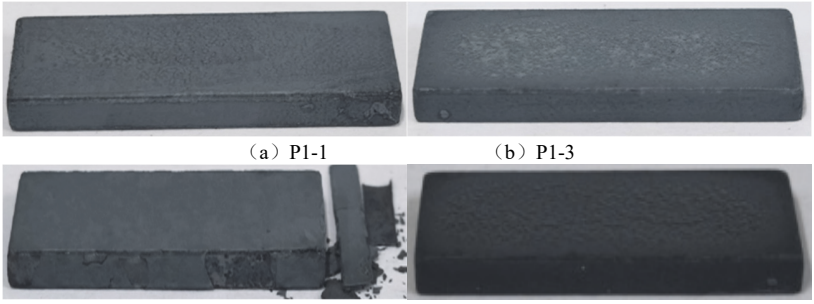

Fig. 2 Surface quality of samples after oxidation and weight gain (a)22MnB5, (b)1.1Si, (c)1.0Cr, (d)1.0Ni.

In the stage II, building upon the findings of the stage I, the content of Si element was further increased to 1.8%, and different contents of Cr, Mo and Cu were introduced to explore the combined influence of elements on the oxidation resistance of the material. The composition design of stage II is shown in Table 2, the results of oxidation experiment are shown in Fig 3, and the surface quality of the oxidized sample is shown in Fig 4.

Table 2 Compositional design list of influencing factors of multi-alloy elements (wt.%)

Number	C	Si	Mn	Al	Cr	B	Ti	Mo	Cu
P2-1	0.24	1.8	1.32	0.031	0.6	0.0021	0.031	0	0
P2-2	0.24	1.8	1.32	0.031	1.0	0.0021	0.031	0	0
P2-3	0.24	1.8	1.32	0.031	0	0.0021	0.031	0.2	0
P2-4	0.24	1.8	1.32	0.031	0	0.0021	0.031	0.4	0
P2-5	0.24	1.8	1.32	0.031	0	0.0021	0.031	0	0.05
P2-6	0.24	1.8	1.32	0.031	0	0.0021	0.031	0	0.3
P2-7	0.24	1.8	1.32	0.031	0	0.0021	0.031	0	0.7

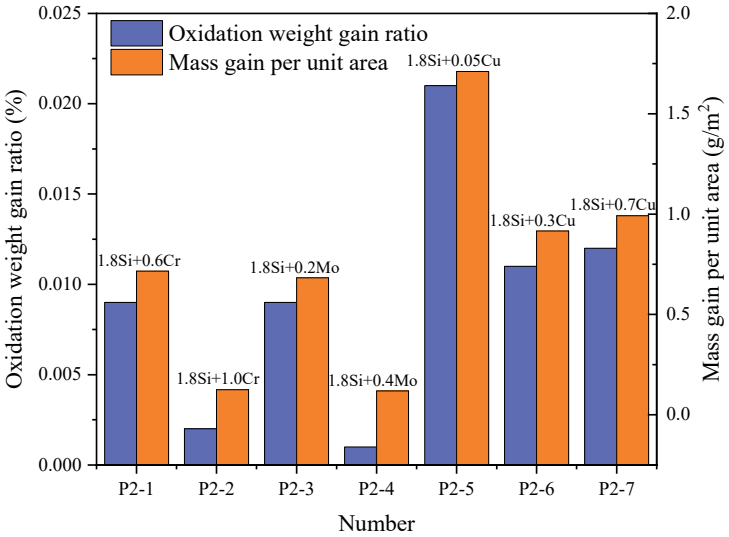

Fig. 3 Oxidation weight gain ratio of multi-alloy elements (Holding temperature: 930 ℃; Heat preservation time: 5 min; Atmosphere: air)

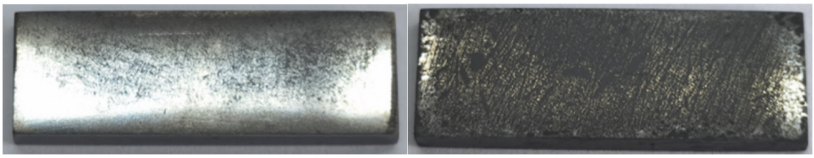

（a）P2-2 （b）P2-4

Fig. 4 Surface state after experiment (a)1.8Si+1.0Cr, (b)1.8Si+0.4Mo.

The experimental results of the stage II show that multi-element composite oxidation weight gain ratio is significantly lower than that of individual element. Specifically, Si combined with other elements exhibits notable improvements in oxidation resistance, particularly the combination of Cr and Mo with Si. For instance, the oxidation weight gain ratio of 1.8Si+1.0Cr is about 0.002%, with an oxidation weight gain per unit area of about 0.125 g/m^2. Meanwhile, the oxidation weight gain ratio of 1.8Si+0.4Mo is about 0.001%, with an oxidation weight gain per unit area of about 0.119 g/m^2. While, both the component

combinations showed excellent oxidation resistance, the surface of P2-4 (1.8Si+1.0Mo) appears black with discolored oxide layer was, whereas P2-2 (1.8Si+1.0Cr) exhibits uniform surface quality with metallic luster. In addition, the price of Mo powder is about 300 yuan/kg, and the price of Cr powder is about 110 yuan/kg. Considering the cost-effective composition design principle, 1.8Si+1.0Cr is finally selected as the optimal composition design.

3.2. *Oxidation kinetics analysis*

The TGA oxidation weight gain experiment was carried out on the material composition sample established in Section ***3.1***, alongside22MnB5, and the oxidation weight gain-time curve per unit area of the material was shown in Fig 5. The results show that under the same conditions, the oxidation weight gain of the design composition sample is about 1.71 mg/cm^2 at the end of heat preservation, representing an 88 % reduction compared to 13.93 mg/cm^2 for 22MnB5. Throughout the heating stage, no obvious changes were observed in the early stage of oxidation, with noticeable oxidative weight gain appearing around 850 ℃, and rapidly increasing as the temperature reaching 950 ℃. During 30-min temperature holding stage, the oxidation weight gain curve of 1.8Si+1.0Cr is parabolic, indicating that a dense layer is formed on its surface that hinders the further oxidation of the matrix[12, 13]. The oxidation kinetics model established according to *Kofstad* (formula 3) is expressed as：

$$(\Delta W)^2 = K_p \tau \quad \text{(Eq 3)}$$

In this Eq.3, ΔW is oxidation weight gain per unit area, in mg/mm^2; τ is oxidation time, in min; K_p is a constant of oxidation rate. Therefore, we can calculate the K_p of 22MnB5 in the condition of 950 ℃ for 30 min is 6.68 mg^{2}cm^{-4}min^{-1}, 1.8Si+1.0Cr is 0.09883 mg^{2}cm^{-4}min^{-1} in the same condition. The fitting degrees of both are above 0.99. It can be concluded that the oxidation rate constant of 1.8Si+1.0Cr is about two orders of magnitude smaller than that of 22MnB5 at 950 ℃ for 30min. All the above results show that the antioxidant properties of 1.8Si+1.0Cr are better than those of 22MnB5, which is consistent with the results of ***3.1***.

3.3. *Phase analysis*

The phase analysis of the surface oxide layer of the TGA experimental sample of 1.8Si+1.0Cr in Section ***3.2*** was carried out, and the XRD pattern extending from the surface to the matrix was obtained. The analysis results are shown in Fig 6. These results show that after the oxidation experiment at 950 ℃+30 min, the oxide layer on the surface of 1.8Si+1.0Cr comprises Fe_2O_3, and the diffraction peak of Fe element indicates that X-ray diffraction reaches the matrix. The analysis shows that the presence of Fe-Si/Cr-O compounds such as Fe_2SiO_4 and $FeCr_2O_4$[14, 15], within the surface oxide layer. These compounds exhibit a spinel structure like Fe_3O_4, characterized by a cubic crystal system, wherein ions are densely packed and arranged, resulting in a compact crystal structure.

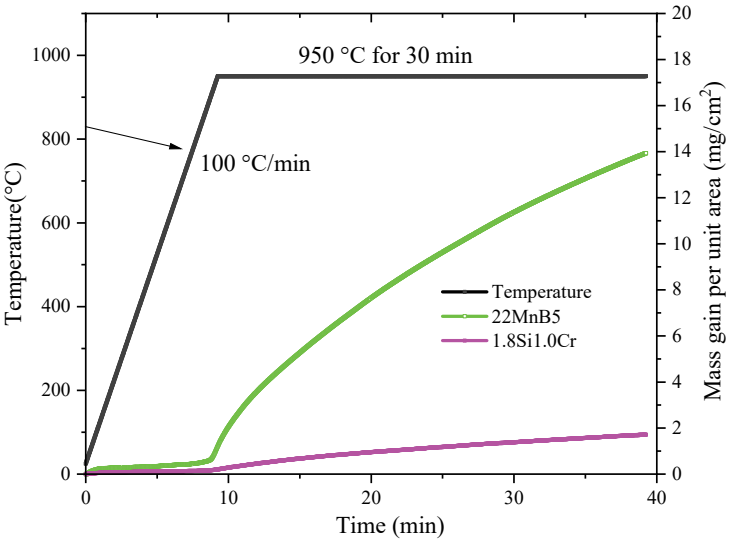

Fig. 5 TGA experimental results (Heating rate: 100k/min; Holding temperature: 930℃; Heat preservation time: 30min; Atmosphere: air)

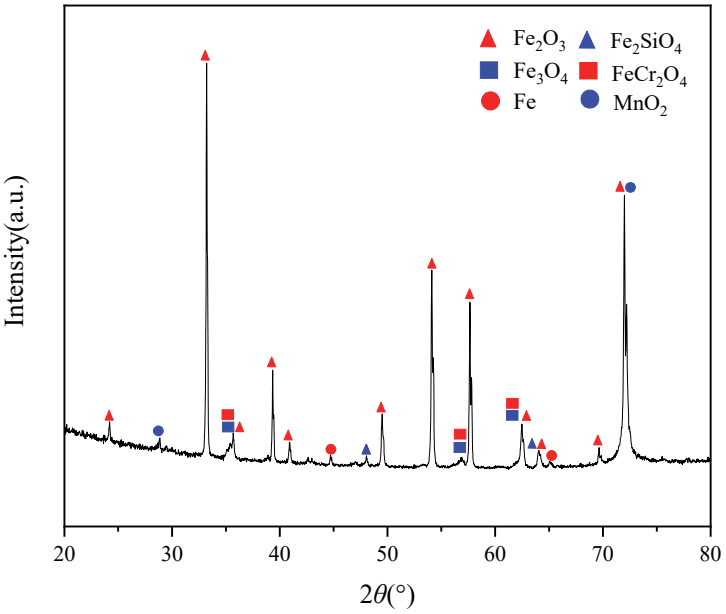

Fig. 6 XRD energy spectrum analysis of oxide layer of TGA experimental sample of 1.8Si+1.0Cr

3.4. *Microstructure analysis of oxide layer*

The TGA experimental samples discussed in Section ***3.2*** were characterized by cross-section microstructure and elemental analysis, and the characterization results are shown

in Figure (7-9). According to the characterization results, after oxidation experiment at 950 ℃+30 min, the thickness of 22MnB5 oxide layer is about 156 μm, showing obvious layered structure, and the oxide layer I is relatively dense, and the oxide layer II is loose and easy to fall off; The thickness of 1.8Si+1.0Cr oxide layer is about 5 μm, and the oxide layer is also layered, and its oxide layer II is thin and closely combined with the matrix. The EDS results show that the oxide layer of 22MnB5 primarily consisted of Fe-O compound, whereas oxide layer II near the matrix is rich in Si-Cr. and the O element does not penetrate into the matrix, but the Fe element diffuses fully. The oxide layer II with 1.8Si+1.0Cr also has obvious enrichment of Si and Cr elements, and oxygen elements are blocked on the surface of the matrix, indicating that the enriched layer effectively prevents the infiltration of oxygen elements. The thickness of 1.8Si+1.0Cr oxide layer Ⅰ is much thinner than 22MnB5, which indicates that the external diffusion of Fe element is hindered, limiting its contact with air. Therefore, the Si-Cr-rich layer formed on the surface of 1.8Si+1.0Cr at high temperature oxidation stage is considered the main factor contributing to its enhanced oxidation resistance.

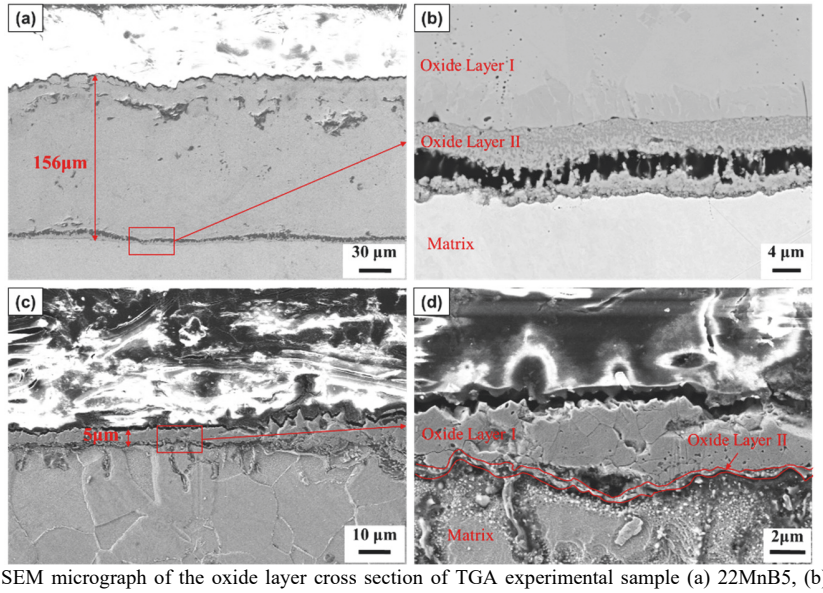

Fig. 7 SEM micrograph of the oxide layer cross section of TGA experimental sample (a) 22MnB5, (b) is an enlarged view of (a) red box area; (c)1.8Si+1.0Cr, and (d) is an enlarged view of (c) red box area.

According to the intensity of XRD diffraction peak and the distribution of EDS elements, it is inferred that the oxide layer I in Fig 7(d) comprises Fe_2O_3, while the oxide layer II is Fe_2SiO_4+$FeCr_2O_4$ composite oxide. Research indicates that following oxidation of 22MnB5 at 950°C for 30 minutes, FeO is the primary oxide layer component. This progressive reaction process involves the initial formation of FeO when Fe diffuses outward, followed by full reaction with O to form Fe_2O_3, with a transition zone of FeO+Fe_2O_3 (i.e., Fe_3O_4) in between. However, the dense oxide layer formed on the surface

of 1.8Si+1.0Cr impedes the Fe diffusion, leading to the formation of substantial Fe_2O_3 in the absence of significant FeO presence in the XRD results. This result further proves that the Si-Cr enrichment layer has a positive effect on improving oxidation resistance[16, 17].

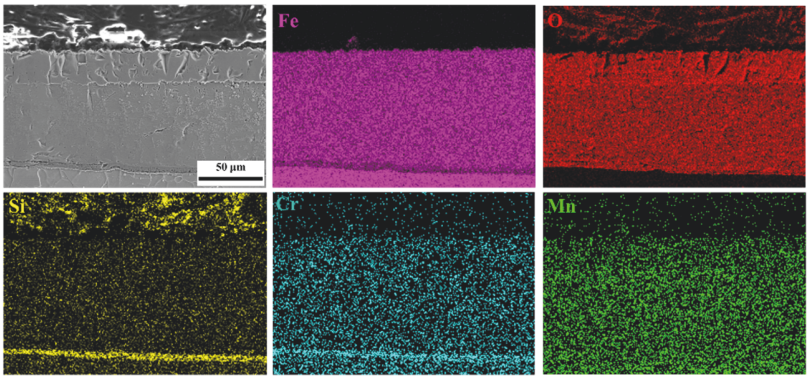

Fig. 8 EDS energy spectrum analysis of oxide layer cross section of 22MnB5 TGA experimental sample.

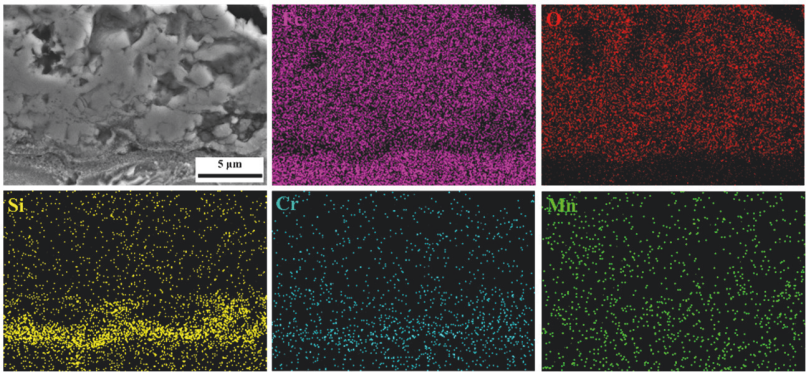

Fig. 9 EDS energy spectrum analysis of oxide layer cross section of 1.8Si+1.0Cr TGA experimental sample.

4. Conclusion

(1) The order of the influence of alloying elements on the antioxidant capacity of 22MnB5 is Si > Cr > Ni.

(2) Based on the principle of low cost and short-term oxidation, the composition ratio of 1.8Si+1.0Cr is preferred.

(3) Following oxidation at 950 ℃ for 30 min, the oxidation weight gain curve of 1.8Si+1.0Cr exhibits a parabolic trend, with noticeable Si and Cr enrichment observed at the interface between the matrix and the oxide layer. Through phase analysis, the enrichment layer primarily consists of Fe2SiO4 and FeCr2O4 spinel, effectively impeding the outward diffusion of Fe ions and the inward diffusion of O ions, thus improving the high-temperature oxidation resistance of PHS.

The significance of this paper lies in significantly improving the high-temperature oxidation resistance of 22MnB5 through the addition of oxidation resistance elements and

thoroughly analyzing its oxidation resistance mechanism. This work provides insights for designing a new type of uncoated and oxidation-resistant PHS.

References

1. N. Ma, Material Performance of Hot-forming High Strength Steel and Its Application in Vehicle Body, Journal of Mechanical Engineering, Vol. 47, no. 08 (2011), Doi: 10.3901/jme.2011.08.060.
2. N. Ma, Research on Boron Steel for Hot Forming and Its Application, Journal of Mechanical Engineering, vol. 46, no. 14 (2010), Doi: 10.3901/jme.2010.14.068.
3. M. R. de Castro, W. A. Monteiro, and R. Politano, Enhancements on strength of body structure due to bake hardening effect on hot stamping steel, The International Journal of Advanced Manufacturing Technology, vol. 100, no. 1-4, pp. 771-782 (2018), Doi: 10.1007/s00170-018-2542-4.
4. Z. Gui, W. Liang, and Y. Zhang, Enhancing ductility of the Al-Si coating on hot stamping steel by controlling the Fe-Al phase transformation during austenitization, Science China Technological Sciences, vol. 57, no. 9, pp. 1785-1793 (2014), Doi: 10.1007/s11431-014-5576-3.
5. M. K. Ji, H. Son, J. Oh, S. Kim, K. Kim, and T.-S. Jun, Effects of Al-Si Coating Thickness on 22MnB5 in Hot Stamping Wear, Korean Journal of Metals and Materials, vol. 58, no. 8, pp. 573-582 (2020), Doi: 10.3365/kjmm.2020.58.8.573.
6. M. Zandrahimi, J. Vatandoost, and H. Ebrahimifar, Al, Si, and Al–Si Coatings to Improve the High-Temperature Oxidation Resistance of AISI 304 Stainless Steel, Oxidation of Metals, vol. 76, no. 3-4, pp. 347-358 (2011), Doi: 10.1007/s11085-011-9259-1.
7. H. Wang, Q. Zhao, H. Yu, Z. Zhang, H. Cui, and G. Min, Effect of aluminium and silicon on high temperature oxidation resistance of Fe-Cr-Ni heat resistant steel, Transactions of Tianjin University, vol. 15, no. 6, pp. 457-462 (2009), Doi: 10.1007/s12209-009-0079-1.
8. Z. Li, L. Wang, Z. Wang, T. Zhang, J. Wang, and W. Xu, Oxidation mechanisms of a Cr Si alloyed coating-free press-hardened steel under simulated press hardening conditions, Materials Characterization, vol. 206 (2023), Doi: 10.1016/j.matchar.2023.113446.
9. T. Zhang, L. Wang, Z. Li, L. Wang, F. Wang, and W. Xu, High-Temperature Oxidation Behavior of Cr-Si Alloyed Press-Hardened Steel in Comparison with 22MnB5 Steel, steel research international, vol. 95, no. 4 (2024), Doi: 10.1002/srin.202300565.
10. C. Zhang et al., Effect of Mo on the high-temperature oxidation behavior of Cr-Ni-Mo hot-work die steels, Corrosion Science, vol. 224 (2023), Doi: 10.1016/j.corsci.2023.111487.
11. D. Biao, Y. Hongliang, and W. Guodong, Effect of Mo on high temperature oxidation behavior of 22MnB5 steel sheet during hot stamping, Steel Rolling, vol. 37, no. 5, pp. 6-11 (2020), Doi: 10. 13228/j. boyuan. issn1003-9996. 20190163.
12. B. Li, Y. Chen, X. Zhao, J. Li, C. Wang, and M. Wang, Effect of Austenitization Process on Oxidative Decarbonization Behavior and Mechanical Properties of 22MnB5 Steel, Journal of Materials Engineering and Performance, vol. 33, no. 1, pp. 213-226 (2023), Doi: 10.1007/s11665-023-07985-4.

13. Y. Wu, Q. Zhang, R. Zhu, M. Wang, H. Jiang, and Z. Mi, Studying the Effect of Cr and Si on the High-Temperature Oxidation-Resistance Mechanism of Hot Stamping Steel, Metals, vol. 13, no. 10 (2023), Doi: 10.3390/met13101670.
14. D. Santamaria-Perez et al., Metastable structural transformations and pressure-induced amorphization in natural (Mg,Fe)2SiO4olivine under static compression: A Raman spectroscopic study, American Mineralogist, vol. 101, no. 7, pp. 1642-1650 (2016), Doi: 10.2138/am-2016-5389CCBY.
15. H. K. Mehtani, M. I. Khan, B. N. Jaya, S. Parida, M. J. N. V. Prasad, and I. Samajdar, The oxidation behavior of iron-chromium alloys: The defining role of substrate chemistry on kinetics, microstructure and mechanical properties of the oxide scale, Journal of Alloys and Compounds, vol. 871 (2021), Doi: 10.1016/j.jallcom.2021.159583.
16. C.-W. Yang, J.-H. Kim, R. E. Triambulo, Y.-H. Kang, J.-S. Lee, and J.-W. Park, The mechanical property of the oxide scale on Fe–Cr alloy steels, Journal of Alloys and Compounds, vol. 549, pp. 6-10 (2013), Doi: 10.1016/j.jallcom.2012.09.064.
17. W. Du, C. Liu, and Y. Yue, Effect of passivation on the high-temperature oxidation behavior of hot-formed steel, Corrosion Science, vol. 202 (2022), Doi: 10.1016/j.corsci.2022.110318.